

## Effect of La and Ce on the catalytic performance of ZSM-5 with the optimal Si/Al ratio in the HTO process

Maryam Ghazimoradi<sup>1</sup>, Saeed Soltanali<sup>2\*</sup>, Nasser Safari<sup>1</sup>, Hamid Kiarad<sup>2</sup> and Hamid Karami<sup>2</sup>

1. Department of Chemistry, Shahid Beheshti University, Tehran, Iran

2. Catalysis Technologies Development Division, Research Institute of Petroleum Industry (RIPI), Tehran, Iran

### Abstract

This study investigates, the performance of ZSM-5 zeolite catalysts with different Si/Al ratios equal to 40, 120, and 200 in the n-hexane catalytic cracking process in a fixed bed microreactor at 550°C under atmospheric pressure with a WHSV = 4 h<sup>-1</sup>. To improve the acidity of the catalysts and increase the yield of light olefins, the best catalyst among the three synthesized catalysts was modified by lanthanum and cerium metals. These two rare earth metals were chosen as modifiers since they were expected to improve the acidic properties of the parent catalyst. Furthermore, XRD, FT-IR, FESEM, EDX Dot-Mapping, BET, and NH<sub>3</sub>-TPD analyses were used to evaluate and characterize the synthesized catalysts. According to the results, the Z-La catalyst has significantly improved catalytic performance, such as the yield of light olefins, P/E ratio, and a decrease in the production of light alkanes and aromatic compounds compared to other catalysts. The yield of light olefins obtained from it was equal to 62.91%, and the P/E ratio was equal to 3.25. This significant progress in this catalyst compared to other catalysts in this research is due to adding La to H-ZSM-5 zeolite, which causes changes and modifies the acidity properties of this catalyst (S/W ratio of acidity = 0.54).

**Keywords:** Catalytic Cracking, ZSM-5 Zeolite, Light Olefins, Lanthanum and Cerium.

### Introduction

Ethylene and propylene as light olefins are the most important bases of the petrochemical industry. In recent decades, the demand for light olefins, especially propylene, as critical raw materials for chemical industry use, has increased exponentially. Due to the increasing demand for light olefins worldwide and in Iran, producing these valuable materials from domestic oil and gas sources will reduce foreign dependence [1–5]. Propylene has been produced as a by-product along with ethylene from naphtha cracking units. Considering the existing gap between the production and demand of the propylene market worldwide and the much higher demand for propylene, the current productions with the thermal cracking method are not responsive. Also, the thermal cracking method is not environmentally friendly. For example, it consumes much energy and emits much carbon dioxide into the atmosphere [6–8]. Light olefins with higher selectivity will be obtained in the alternative thermal cracking reaction, which is the catalytic cracking of naphtha at a much lower temperature than thermal cracking. Among the used zeolite catalysts, ZSM-5 zeolite has shown more activity, catalytic performance, and hydrothermal stability in the catalytic cracking

process, which is due to its acidic properties and specific morphology [9,10]. Also, this zeolite catalyst has high selectivity due to its shape selectivity-based property. Although among the various catalysts used in the catalytic cracking process, ZSM-5 had the best performance, the yield of light olefins produced using this catalyst is very low. During the long-term reaction, the catalytic activity and lifetime of ZSM-5 decrease significantly with coke formation. The origin of coke is aromatic molecules (BTX) in the catalytic cracking reaction [11,12]. After the formation of aromatic molecules, most of these aromatic substances are released from the microcrystals in the pores and released as BTX products. At the same time, a small part of them remain in the zeolite micropores as coke precursors and form coke [13–15]. By increasing the reaction time, all the pores with active acid sites are blocked, which results in a significant decrease in the catalytic activity, conversion, and production of light olefins [16]. In this research, ZSM-5 zeolites were synthesized with three Si/Al ratios of 40, 120, and 200 (Z-40, Z-120, and Z-200), and they were compared in terms of catalytic performance. Finally, to increase the yield of light olefins, the best catalyst among these three prepared samples (Z-120) was modified by two metals,

\*Corresponding author: Saeed Soltanali, Catalysis Technologies Development Division, Research Institute of Petroleum Industry (RIPI), Tehran, Iran

E-mail addresses: [soltanalis@ripi.ir](mailto:soltanalis@ripi.ir)

Received 2024-01-21, Received in revised form 2024-01-22, Accepted 2024-01-22, Available online .....



lanthanum and cerium, using the impregnation method. These two rare earth metals were chosen as modifiers since they were expected to improve the acidic properties of the parent catalyst. It was illustrated by Wang et al. [17] that the use of RE elements in the H-ZSM-5 sample not only modified the number of acid sites of H-ZSM-5 but also altered the acid strength and type. They showed the significant impact of acidity properties after using RE elements on the catalytic performance of H-ZSM-5. In another study [18], Ce and Zr loading could promote ethylene and propylene yield in the catalytic cracking of naphtha. Also, the effect of lanthanum metal as a rare metal was investigated in previous studies. For example, cerium and lanthanum impregnated on SAPO-34 were synthesized and used in catalytic cracking of naphtha to produce light olefins [19].

In this research, the effects of this modification method were investigated on the acidic and textural characteristics of zeolite samples, and different catalysts were characterized using XRD, FT-IR, FESEM, EDX Dot-Mapping, BET, and NH<sub>3</sub>-TPD analyses. In the end, the prepared catalysts' HTO (hexane to olefins) performance was investigated using a microreactor system.

## Materials and Methods

### Chemicals Materials

The materials used for the synthesis of catalysts include colloidal silica (40 wt% SiO<sub>2</sub>, Aldrich), Aluminum sulfate (Al<sub>2</sub>(SO<sub>4</sub>)<sub>3</sub>.18H<sub>2</sub>O, Merck Co, Germany), respectively as sources of silicon and aluminum, tetrapropylammonium hydroxide (TPAOH, Merck Co, Germany), Sodium hydroxide (NaOH), Cerium nitrate (Ce(NO<sub>3</sub>)<sub>3</sub>.6H<sub>2</sub>O), and lanthanum nitrate (La(NO<sub>3</sub>)<sub>3</sub>.6H<sub>2</sub>O), and ammonium nitrate (NH<sub>4</sub>NO<sub>3</sub>, Merck Co, Germany).

### Catalyst Preparation

Na-ZSM-5 zeolite catalysts were prepared, by hydrothermal method and according to the basic formula 00SiO<sub>2</sub>:xAl<sub>2</sub>O<sub>3</sub>:15TPAOH:19NaO<sub>2</sub>:3200H<sub>2</sub>O (x = 7.5, 2.5, 1.25 respectively for Si/Al ratios equal to 40, 120, and 200) and were named as Z-40, Z-120, and Z-200 respectively. Firstly, to prepare zeolites according to the basic formula for each ratio, a certain amount of aluminum sulfate was dissolved in distilled water and sodium hydroxide (Solution No. 1). Solution No. 2 also contains a mixture of colloidal silica and TPAOH. After dissolving both solutions separately, solution 1 was added to solution 2. After that, 3 wt.% of seed was added to the mixture and it was stirred to obtain a homogenous solution. Next, the beaker's contents were transferred to the autoclave and placed in a stirring oven for 72 h at 180 °C. After 72 hours, the autoclave was cooled down slowly at room temperature. Then, the contents inside the autoclave were filtered and washed until the pH of the solution under the filter reached about 7. After reducing the pH, the samples were dried at 100 °C for 12 h, and transferred to an electric furnace with a temperature of 550 °C for 4 h to perform the calcination process. Next, to convert the sodium form into the protonic form of zeolite ZSM-5, ion exchange was performed with 2M ammonium nitrate solution 3 times and 3 h each time. Next, to improve the catalyst's performance with

an optimal ratio regarding reactor test performance, Z-120 zeolite was modified with cerium and lanthanum metals by the dry impregnation method. The impregnation solution for catalysts was synthesized with 2% wt of cerium and 2% wt of lanthanum. After impregnation, catalysts were dried at 100 °C. After that, the catalyst was calcined at 550 °C for 4 hours. These two samples were named Z-Ce and Z-La.

### Catalyst Characterization

The synthesized catalysts, X-ray diffraction analysis using an X-ray diffractometer, Theta-Theta model (Stoe Co) was used with a Cu K $\alpha$  lamp ( $\lambda=1.5406 \text{ \AA}$ ) in  $2\theta=5-55^\circ$  with a step size  $0.06^\circ$  and 1s to determine the phase and crystallinity of the synthesized catalysts. To identify the structural changes in the prepared samples, Bruker model IR device manufactured by PerkinElmer Germany was used and this analysis was performed in the range of 400-4000 wavenumber with a wavelength of  $1 \text{ cm}^{-1}$ . The morphology of particles and crystals in zeolite samples was performed using scanning electron microscopic analysis (FE-SEM, ZEISS Co, Germany) Sigma VP model. With this device, EDX Dot-Mapping analysis was done to determine the elemental composition of the samples and the abundance distribution of the elements. Micromeritics ASAP2000 device was used to calculate the average size and volume of the pores, and the surface area of the prepared samples, using N<sub>2</sub> adsorption-desorption isotherm (Brunauer-Emmett-Teller). Before carrying out the nitrogen adsorption and desorption tests, the samples were vacuumed for 12 h at 300°C and degassed to separate the molecules adsorbed on the surface. Then the tests were performed at a temperature of -196°C. NH<sub>3</sub>-temperature programmed desorption was analyzed using the Micromeritics TPR/TPD 2900 device to calculate the amount and strength of acid sites. In this analysis, the amount and strength of acidic sites were determined by using the area under the peak of the NH<sub>3</sub>-TPD profile and the position of the peaks, respectively.

### Performance Evaluation System of Prepared Catalysts

The fixed bed reactor system was used as shown in Fig. 1, to evaluate the performance of the synthesized catalysts in the n-hexane catalytic cracking process. In each reactor test, 0.67 g of catalyst and 0.33 g of quartz were loaded in the reactor reaction area to dilute the catalysts. The reactor reaction was carried out at 550°C under atmospheric pressure with a WHSV=4 h<sup>-1</sup>. At first, the flow of N<sub>2</sub> was established with a flow rate of 40 cc/min through a mass flow controller (MFC), and the catalyst bed was heated to 550 °C under an N<sub>2</sub> flow. The mass flow rate and the reactor temperature controllers are controlled by the four-channel power supply, display, and controller. After the temperature of the catalyst bed reached 550°C, the reactor system remained in this condition for half an hour. A few minutes after stabilizing the conditions, the n-hexane flow rate (0.068 cc/min) was introduced in the reactor using a syringe pump and after passing the n-hexane flow rate through the preheater area, the output flow rate from the reactor was measured, and recorded immediately. The gaseous product samples were collected every half hour for injection into the gas chromatography (GC) instrument (Agilent), which was equipped with FID and TCD detectors.

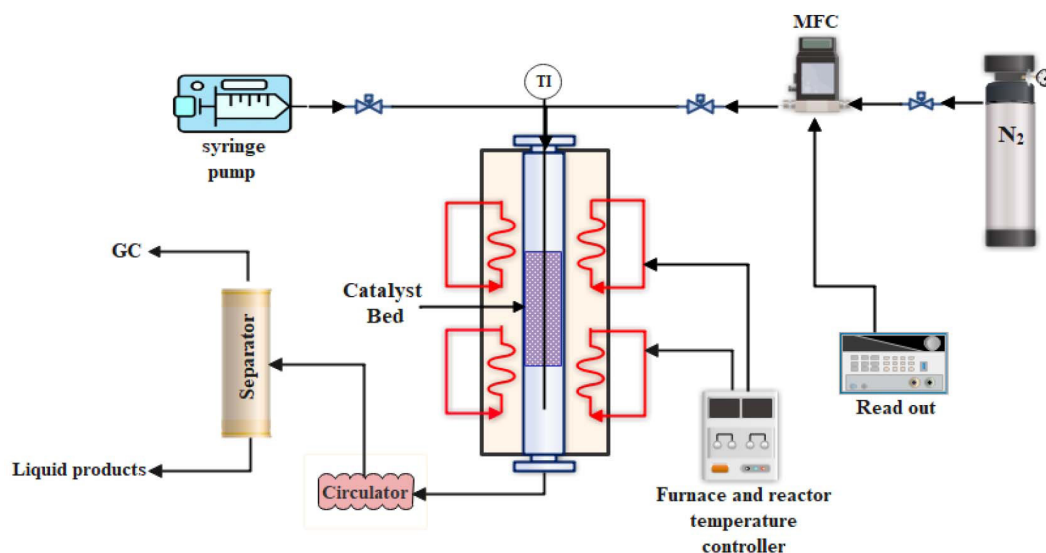


Fig. 1 Laboratory system for catalysts performance tests in HTO process.

After injecting the last GC sample, the feed flow was stopped and the liquid sample was collected for analysis. N-hexane conversion, product selectivity, and yield of light olefins are calculated by equations 1, 2, and 3. ( $X$ ,  $S_i$ , and  $i$  are conversion, selectivity, and each product)

$$X_{(n\text{-hexane})} = \frac{(n\text{-hexane})_{\text{inlet}} - (n\text{-hexane})_{\text{out}}}{(n\text{-hexane})_{\text{inlet}}} * 100\% \quad (1)$$

$$S_i = \frac{n_{i,\text{out}}}{\sum n_{i,\text{out}}} * 100\% \quad (2)$$

$$\text{Yield } i = \text{selectivity } i * \text{conversion } i \quad (3)$$

## Results and Discussion

### Catalyst Characterization

The synthesized samples were investigated and identified by XRD, FT-IR, FESEM, EDX Dot-Mapping, BET, and  $\text{NH}_3$ -TPD methods, which are discussed below.

### XRD Analysis

The XRD patterns of all the synthesized catalysts are shown in Fig. 2. In this figure, the comparison of the X-ray diffraction data of the synthesized H-ZSM-5 zeolites and data of the standard sample of this zeolite (card number: JCPDS No. 00-044-0003) in the IZA (International Zeolite Association) reference is seen. This comparison shows the presence of pure and crystalline phases of the synthesized H-ZSM-5 zeolite in the crystal structure of this sample [20]. The ZSM-5 zeolite index peaks are:  $2\theta = 7.95^\circ$ ;  $8.84^\circ$ ;  $23.09^\circ$ ;  $23.32^\circ$ ;  $23.93^\circ$ . The results of the XRD analysis show that the synthesized zeolites have no amorphous phase and a good crystal structure. This result is obtained from the high intensity of the main peaks. Also, according to the XRD pattern of Z-Ce and Z-La, it can be concluded that the dispersion of metals is completely uniform and homogeneous on the catalyst and no new peaks related to metal oxides were observed in any of the samples. There were no adverse effects, such as collapse or amorphization of the zeolite crystal structure.

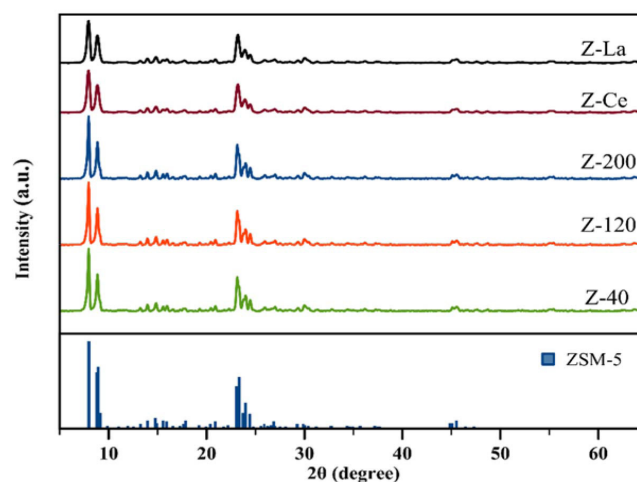


Fig. 2 XRD pattern of the synthesized samples.

### FT-IR Spectra

According to Fig. 3, the vibrations of the synthesized samples are observed in the spectral region of  $400\text{-}4000\text{ cm}^{-1}$ . The vibrations of the ZSM-5 zeolite framework have seven absorption bands at wave numbers  $453$ ,  $547$ ,  $802$ ,  $1101$ ,  $1225$ ,  $1640$ , and  $3400\text{ cm}^{-1}$ . Asymmetric stretching vibrations that prove the existence of ZSM-5 zeolite crystal structure with a pair of pentagonal rings at  $547\text{ cm}^{-1}$ , Bending vibrations of T-O bonds (T: Si, Al) related to  $\text{SiO}_4$  and  $\text{AlO}_4$  tetrahedral units at  $453\text{ cm}^{-1}$ , symmetric stretching vibrations of T-O bonds at  $802\text{ cm}^{-1}$  and asymmetric stretching vibrations of T-O bonds at  $1104\text{ cm}^{-1}$  are seen in Fig. 3. The absorption bond near  $1225\text{ cm}^{-1}$  is related to external asymmetric stretching vibrations and indicates the existence of H-ZSM-5 crystal structures consisting of four five-membered rings arranged around the two-dimensional torsion axis [10,21]. The presence of all these vibrations in the mentioned spectral regions in all prepared zeolites indicates that the ZSM-5 zeolite framework structure has been completely preserved after synthesis and impregnation, and the collapse of the structure is not observed.

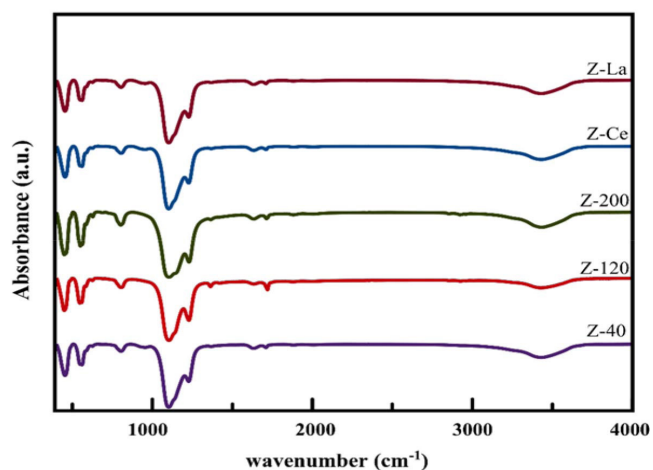


Fig. 3 FT-IR profile of synthesized samples.

### FE-SEM and EDX Dot-Mapping Analyses

In Fig. 4, the FE-SEM images of prepared zeolite samples shown. As shown in Fig. 4, the synthesized samples comprise uniform nanocrystals with the same morphology. Z-40 and Z-120 samples have a hexagonal (coffin) structure, and Z-200 sample has a special polyhedral structure [6]. According to the FE-SEM images recorded of Z-Ce and Z-La samples, it can be seen that the dispersion of metals on these zeolites is completely homogeneous and uniform on the structure of Z-120 zeolite. It indicates that metals do not affect the particles of zeolite [22]. According to Fig. 5, EDX Dot-Mapping analyses show that the dispersion of 2 metals after the impregnation process performed perfectly in the two Z-Ce and Z-La samples, and according to the available related Mappings, there is no observed accumulation or aggregation of metals that indicates dispersion is weak.

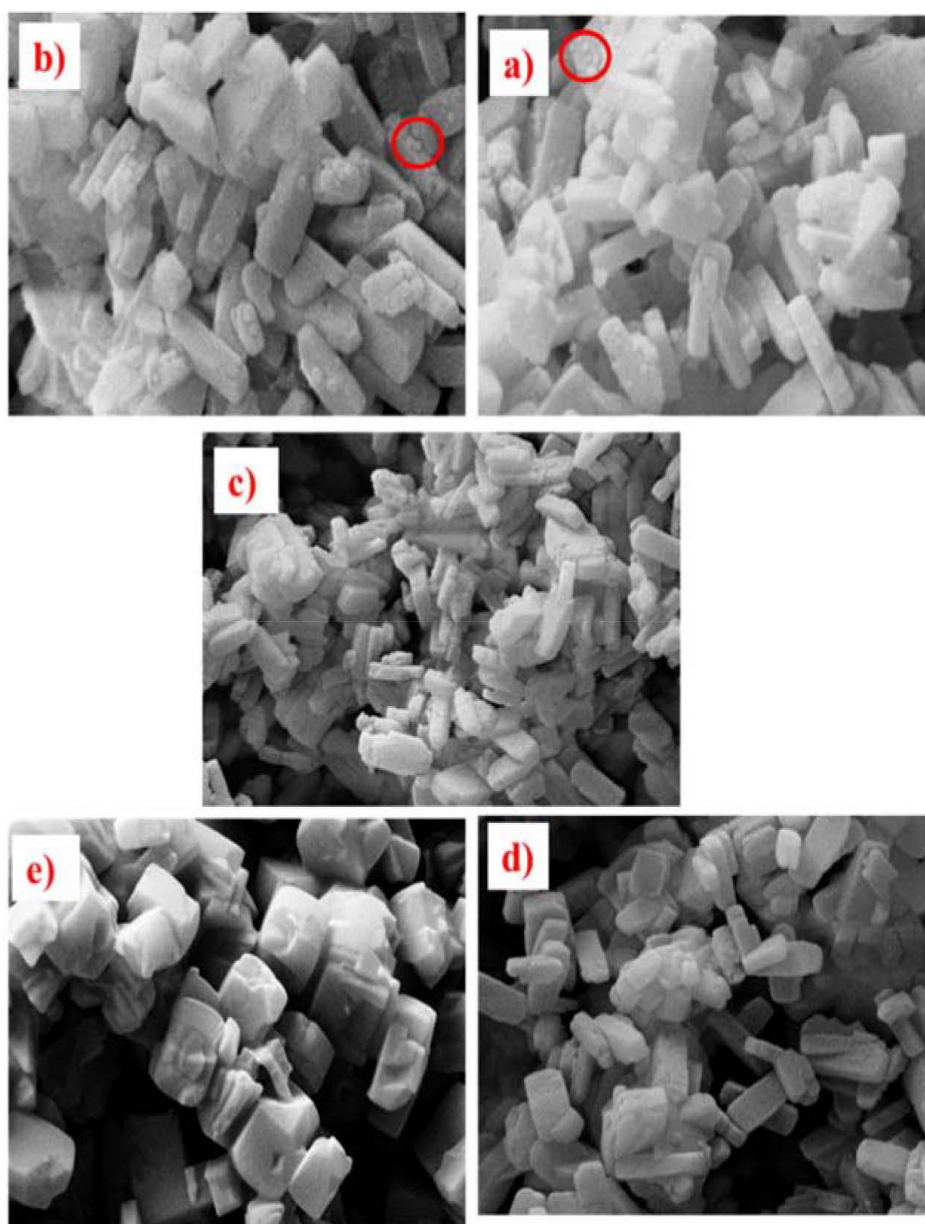
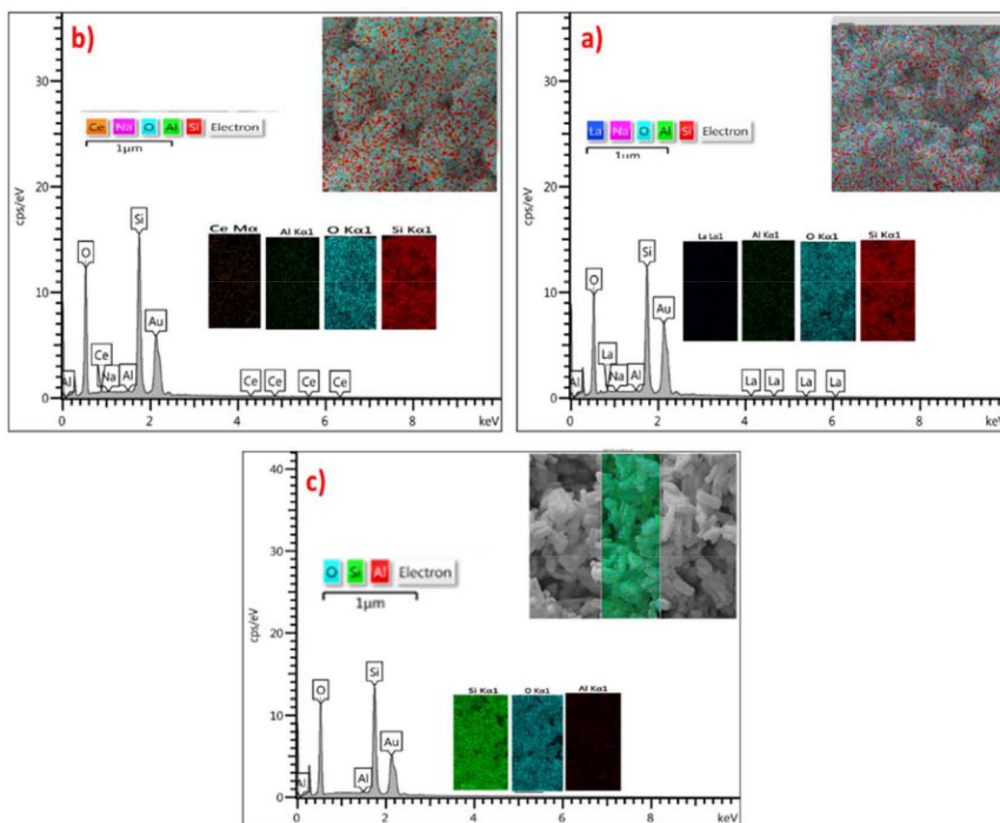


Fig. 4 FE-SEM images of catalytic samples a) Z-La, b) Z-Ce, c) Z-120, d) Z-40, e) Z-200.





**Fig. 5** The results of EDX-dot-mapping analysis, a) Z-La, b) Z-Ce, c) Z-120.

#### Nitrogen Adsorption-desorption (BET) Tests

Adsorption and desorption isotherms of prepared ZSM-5 zeolite samples are shown in Figure. 6. It is obvious that all nitrogen adsorption and desorption curves have type IV isotherms based on the classification provided by the International Union of Pure and Applied Chemistry (IUPAC) [23–25]. According to the isotherms of each sample in Fig. 6, all available catalytic samples showed high adsorption at low relative pressure. This event proves the presence of micropores

in all the synthesized samples. The presence of hysteresis loops at high relative pressure in all samples confirms the existence of mesopores and capillary condensation in the structure of zeolite samples [26]. According to Table 1, in Z-Ce and Z-La zeolite samples, due to the processing conditions of these catalysts and the addition of active metals due to the filling of pores, the BET surface area, as well as the amount of micro and mesopores compared to the Z-120 catalyst has decreased slightly.

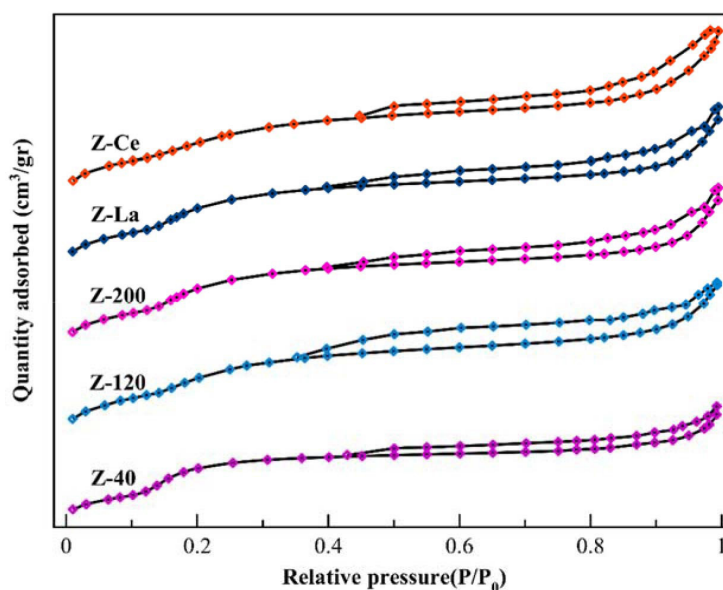


**Fig. 6** Nitrogen adsorption and desorption isotherms.

**Table 1** The results of N<sub>2</sub> adsorption-desorption analysis.

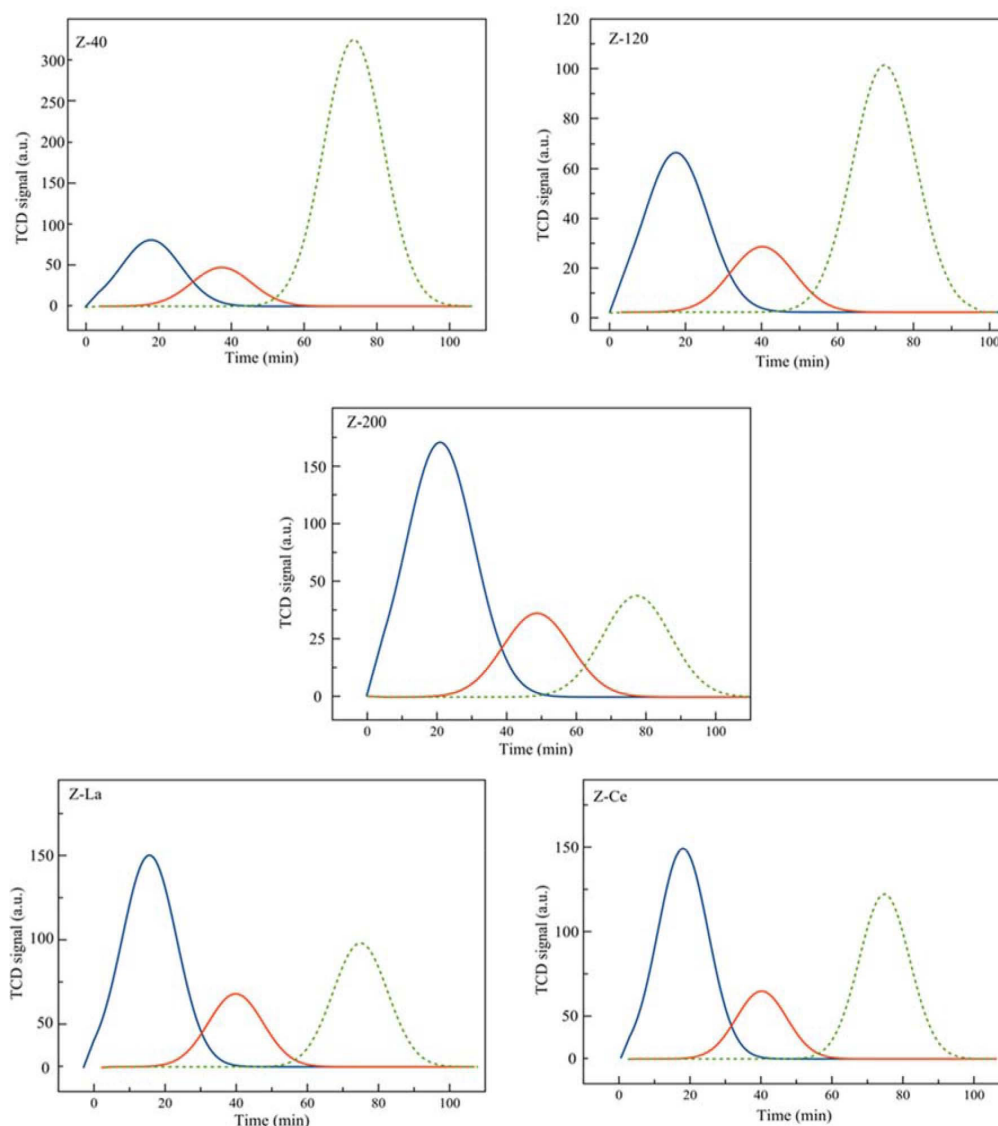
Catalyst	S BET (m <sup>2</sup> /g)	S external (m <sup>2</sup> /g)	V total (cm <sup>3</sup> /g)	V micropore (cm <sup>3</sup> /g)	V mesopore (cm <sup>3</sup> /g)	D (nm)	HF <sup>a</sup>
Z-40	324	110	0.191	0.065	0.126	2.358	0.115
Z-120	374	215	0.287	0.086	0.201	3.069	0.172
Z-200	364	200	0.241	0.069	0.172	2.648	0.157
Z-Ce	355	205	0.265	0.083	0.182	2.985	0.181
Z-La	337	210	0.272	0.081	0.191	3.228	0.185

$$^a \text{HF} = \text{hierarchical factor} = (V_{\text{micro}}/V_{\text{total}})(S_{\text{ext}}/S_{\text{BET}})$$

### Ammonia-temperature Programmed Desorption Analysis

The results of the temperature-programmed desorption analysis for the synthesized zeolite samples are reported in Fig. 7 and Table 2. As seen in Fig. 7, the ammonia desorption profiles for all samples have desorption peaks in three regions: low temperature, medium temperature, and high temperature. These indicate three weak, medium, and strong acid site types for all zeolite samples, respectively. The reason for drastic changes in the amount of acidity for three synthesized zeolites (Z-40, Z-120, Z-200) can be the Si/Al ratio or, more specifically, the number of aluminum, according to which the amount of acidity and strength of acidity will also change

[12,27]. It is said that the smaller the number of aluminum in the zeolite unit cell, the more acid strength increases due to the isolation of aluminum atoms in the zeolite. The amount of total acidity and weak acidity in Z-Ce and Z-La samples has increased compared to their primary zeolite (Z-120) due to the RE compounds, possessing Lewis acidity properties, due to the presence of valence electrons and empty f orbitals in RE elements. Also, the amount of medium acidic sites has increased in them. The increase in medium acid sites is due to the interactions between metal species and inherent acid sites in ZSM-5 zeolite [3,21].

**Fig. 7** NH<sub>3</sub>-TPD profiles of prepared zeolite samples.

**Table 2** NH<sub>3</sub>-TPD analysis results.

Samples	Total acidity	Acidity by NH <sub>3</sub> -TPD (mmol·g <sup>-1</sup> )			Strong acid sites weak acid sites
		weak	medium	Strong	
Z-40	1.76	0.33 (217)	0.08 (347)	1.35 (607)	4.09
Z-120	0.67	0.26 (219)	0.07 (349)	0.34 (609)	1.30
Z-200	0.59	0.38 (225)	0.09 (356)	0.12 (611)	0.31
Z-La	0.89	0.48 (220)	0.15 (351)	0.26 (608)	0.54
Z-Ce	0.85	0.41 (218)	0.13 (350)	0.31 (612)	0.75

### Performance of Synthesized Catalysts

The catalytic cracking performance obtained from the synthesized catalysts in the catalytic cracking process of normal hexane was investigated and it is displayed in Table 3. The main products of the cracking process include light olefins, light alkanes (methane to butane), C4+, and BTX. According to Table 1, the pores' diameter and the mesopores' volume in the Z-La and Z-Ce catalysts are greater than other catalysts except their primary catalyst, which increases the access to active acid sites in these catalysts compared to other samples. The catalytic performance of impregnated samples is better than their parent catalyst, although the Z-120 catalyst has a larger mesopores volume than impregnated catalysts; this can be due to the improvement of the acidic properties of impregnated catalysts compared to their parent catalyst. As shown in Table 3, compared to other catalysts prepared in this research, the Z-La catalyst has the best results regarding light olefins yield, reduction in aromatic compounds production (BTX), and the highest P/E ratio. This sample has better characteristics in terms of acidity and pore size (and the highest amount of mesopores except Z-120 catalyst) and the highest amount of hierarchical factor, one of the most important tools for describing zeolites with meso-micro pores. The highest of this parameter in the impregnated samples compared to the parent sample shows the preservation of more micropores and indicates that the increase in the ratio of mesoporation ( $S_{ext} / S_{BET}$ ) is greater than the decrease in the ratio of microporation ( $V_{mic} / V_{total}$ ) [28]. The selectivity towards the products or the coke formation in the catalytic cracking reaction of hydrocarbons is completely influenced and defeated by the properties of the acid catalyst. Acidic properties have been proven as a tool for modulating catalytic activity, selectivity to propylene, and catalyst stability in catalytic cracking in hydrocarbon reactions. In fact, a stronger relative acidity is required to activate the alkane molecules in the cracking of alkanes. Still, the amount of this acidity must be controlled because, on the other hand, the undesirable secondary reactions of the produced alkenes (hydrogen transfer reactions) also occur on these strong acid sites. With more coke production, the deactivation rate increases rapidly. Modifying of zeolite ZSM-5 with RE metals can moderate the acidity of the catalyst and suppress hydrogen transfer and aromatization reactions [17,29]. According to the obtained results, it can be seen that in the catalysts modified with lanthanum and cerium metals, the increase in the density of weak acidity, which can be attributed to Lewis acids [27] causes a decrease in the ratio of strong to weak (S/W) acid sites in the sample, which has reduced the

hydrogen transfer reactions and as a result increased the yield of light olefins and improved the P/E ratio [9,30]. According to Table 3 and Figure. 8, it can be seen that the decrease in the rate of deactivation and the hydrogen transfer index (HTI) reactions in catalysts are respectively equal to: Z-La < Z-Ce < Z-120 < Z-200 < Z-40, and the amount of production of light olefins and its yield have increased contrariwise. RE elements possess 4f orbitals without full electron occupancy and the lanthanide contraction. Introducing RE<sup>3+</sup> such as La<sup>3+</sup> and Ce<sup>3+</sup>, into zeolites leads to the formation of Lewis acid sites, which are metal ions placed in the tetrahedral structure of zeolite [31,32]. It has also been proven that modifying of zeolites by metal ions creates attractive bifunctional catalysts in which metals play a role in both metal active and acidic sites. As a result, cracking activity and selectivity towards light alkenes are improved by modifying both metal and acid active sites. According to the previous research reported in the literature recently, i.e., the results of n-hexane catalytic cracking reaction revealed that the light olefins selectivities with fluffy-ball like ZSM-5 (47.6%) [33], and another research with optimum catalytic performance with the conversion of 95.5% and light olefins selectivities of 56.7% [34], indicate that the results of the catalytic performance in the present article have improved significantly due to the use of RE<sup>3+</sup> metals.

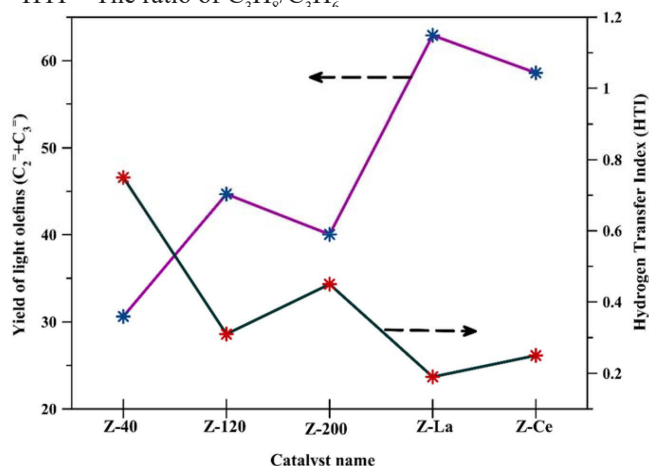
### Conclusions

In this research, the synthesis of ZSM-5 zeolite was done with three different ratios, and the best catalyst among the three synthesized catalysts was modified by lanthanum and cerium metals. Modification by metals causes the preparation of catalysts in which metals play a role in both active metal and acidic sites. As a result, the catalytic performance is improved by modifying both active metal sites and active acid sites. According to the obtained results, it can be seen that in the catalysts modified with lanthanum and cerium metals (Z-La and Z-Ce), the increase in the density of weak acidity, which can be attributed to Lewis acids, has caused a decrease in the ratio of strong to weak acid sites in the samples. It has reduced the hydrogen transfer reactions, and as a result, it has increased the yield of light olefins and improved the P/E ratio. This reduction of S/W in the catalyst containing lanthanum is less than all the samples, and it has a value equal to 0.54, and the hierarchical factor value is equal to 0.185 for the Z-La sample. In this catalyst, the yield of light olefins has reached 62.91%, making significant progress. Therefore, adjusting the acidity is one way to improve the catalytic performance of the zeolite catalysts in the catalytic cracking process.

**Table 3** Distribution of the products obtained from the prepared samples in the HTO process under the mentioned conditions.

Samples	Conversion	C <sub>2</sub> =(%mol)	C <sub>3</sub> =(%mol)	C <sub>4+</sub> =(%mol)	∑(C <sub>1</sub> -C <sub>4</sub> ) (%mol)	Yield (C <sub>2</sub> +C <sub>3</sub> =)	BTX	Rate of De-activation	HTI <sup>a</sup>
Z-40	88.33	13.51	21.15	9.80	52.74	30.61	2.8	14.30	0.75
Z-120	94.58	14.68	32.57	20.31	31.25	44.68	1.2	9.36	0.31
Z-200	92.46	14.32	28.98	12.17	42.63	40.03	1.9	10.31	0.45
Z-La	97.16	15.22	49.53	13.90	21.35	62.91	-	5.42	0.19
Z-Ce	96.09	15.05	46.24	10.08	28.63	58.89	-	7.29	0.25

<sup>a</sup> HTI = The ratio of C<sub>3</sub>H<sub>6</sub>/C<sub>2</sub>H<sub>4</sub>

**Fig. 8** Relevance between HTI amount and yield of light olefins.

## References

- Siddiqui, B., Aitani, A. M., Saeed, M. R., & Al-Khattaf, S. (2010). Enhancing the production of light olefins by catalytic cracking of FCC naphtha over mesoporous ZSM-5 catalyst, *Topics in Catalysis*, 53(19), 1387–1393, doi.org/10.1007/s11244-010-9598-1.
- Nasser, G. A., Kurniawan, T., Tago, T., Bakare, I. A., Taniguchi, T., Nakasaka, Y., Masuda, T., & Muraza, O. (2016). Cracking of n-hexane over hierarchical MOR zeolites derived from natural minerals, *Journal of the Taiwan Institute of Chemical Engineers*, 61, 20–25, doi.org/10.1016/j.jtice.2015.11.025.
- Salah Aldeen, O. D. A., Mahmoud, M. Z., Majdi, H. S., Mutlak, D. A., & Fakhridinovich Uktamov, K. (2022). Investigation of effective parameters Ce and Zr in the synthesis of H-ZSM-5 and SAPO-34 on the production of light olefins from naphtha, *Advances in Materials Science and Engineering*, doi.org/10.1155/2022/6165180.
- Tanimu, A., Tanimu, G., Alasiri, H., & Aitani, A. (2022). Catalytic cracking of crude oil: mini review of catalyst formulations for enhanced selectivity to light olefins, *Energy & Fuels*, 36(10), 5152–5166, doi.org/10.1021/acs.energyfuels.2c00567.
- Al-Shafei, E. N., Aljishi, A. N., Shakoor, Z. M., Albahar, M. Z., Aljishi, M. F., & Alasseel, A. (2023). Steam catalytic cracking and lump kinetics of naphtha to light olefins over nanocrystalline ZSM-5 zeolite. *RSC Advances*, 13(37), 25804–25816, doi: 10.1039/D3RA03157H.
- Hou, X., Qiu, Y., Zhang, X., & Liu, G. (2017). Analysis of reaction pathways for n-pentane cracking over zeolites to produce light olefins, *Chemical Engineering Journal*, 307, 372–381, doi.org/10.1016/j.cej.2016.08.047.
- Kubota, Y., Inagaki, S., & Takechi, K. (2014). Hexane cracking catalyzed by MSE-type zeolite as a solid acid catalyst. *Catalysis Today*, 226, 109–116, doi.org/10.1016/j.cattod.2013.10.032.
- Muraza, O., Bakare, I. A., Tago, T., Konno, H., Taniguchi, T., Al-Amer, A. M., Yamani, Z. H., Nakasaka, Y., & Masuda, T. (2014). Selective catalytic cracking of n-hexane to propylene over hierarchical MTT zeolite. *Fuel*, 135, 105–111, doi.org/10.1016/j.fuel.2014.06.045.
- Ghazimoradi, M., Soltanali, S., Karami, H., Ghassabzadeh, H., & Bakhtiari, J. (2023). A facile strategy to prepare ZSM-5-based composites with enhanced light olefin selectivity and stability in the HTO process. *RSC Advances*, 13(29), 20058, doi.org/10.1039/D3RA03680D.
- Ghazimoradi, M., Soltanali, S., Safari, N., & Ghassabzadeh, H. (2023). Synthesis of fluorinated ZSM-5 catalysts: fluoride effect on structure properties and coke resistance in n-hexane catalytic cracking. *Journal of Materials Science*, 1–17, doi.org/10.1007/s10853-023-08776-x.
- Li, J., Liu, M., Li, S., Guo, X., & Song, C. (2019). Influence of diffusion and acid properties on methane and propane selectivity in methanol-to-olefins reaction. *Industrial & Engineering Chemistry Research*, 58(5), 1896–1905, doi.org/10.1021/acs.iecr.8b03969.
- Zhou, H., Zhang, F., Ji, K., Gao, J., Liu, P., Zhang, K., & Wu, S. (2021). Relationship between Acidity and Activity on Propane Conversion over Metal-Modified HZSM-5 Catalysts. *Catalysts*, 11(10), 1138, doi.org/10.3390/catal11101138.
- Chal, R., Gerardin, C., Bulut, M., & van Donk, S. (2011). Overview and industrial assessment of synthesis strategies towards zeolites with mesopores. *ChemCatChem*, 3(1), 67–81, doi.org/10.1002/cctc.201000158.
- Fals, J., Toloza, C. A. T., Puello-Polo, E., Márquez, E., & Méndez, F. J. (2023). A comprehensive study of product distributions and coke deposition during catalytic cracking of vacuum gas oil over hierarchical zeolites. *Heliyon*, 9(4), doi.org/10.1016/j.heliyon.2023.e15408.
- Abello, S., Bonilla, A., & Perez-Ramirez, J. (2009). Mesoporous ZSM-5 zeolite catalysts prepared by desilication with organic hydroxides and comparison with NaOH leaching, *Applied Catalysis A: General*, 364(1–2), 191–198, doi.org/10.1016/j.apcata.2009.05.055.
- Ahmadpour, J., & Taghizadeh, M. (2015). Catalytic conversion of methanol to propylene over high-silica mesoporous ZSM-5 zeolites prepared by different combinations of mesogenous templates. *Journal of Natural Gas Science and Engineering*, 23, 184–194, doi.org/10.1016/j.jngse.2015.01.035.
- Xiaoning, W., Zhen, Z., Chunming, X., Aijun, D., Li,



- Z., & Guiyuan, J. (2007). Effects of light rare earth on acidity and catalytic performance of HZSM-5 zeolite for catalytic cracking of butane to light olefins. *Journal of Rare Earths*, 25(3), 321–328, doi.org/10.1016/S1002-0721(07)60430-X.
18. Momayez, F., Towfighi Darian, J., & Mohammadalizadeh, A. (2014). The effect of Ce and Zr loading over HZSM-5 to produce light olefins from naphtha, *Nashrieh Shimi va Mohandesi Shimi Iran*, 33(1), 37–47, doi.org/10.1016/j.jaap.2015.02.006.
19. Taghipour, N., Towfighi, J., Mohamadalizadeh, A., Shirazi, L., & Sheibani, S. (2013). The effect of key factors on thermal catalytic cracking of naphtha over Ce–La/SAPO-34 catalyst by statistical design of experiments, *Journal of Analytical and Applied Pyrolysis*, 99, 184–190, doi.org/10.1016/j.jaap.2012.09.008.
20. D5758-01. (2015). Standard test method for determination of relative crystallinity of zeolite ZSM-5 by X-ray diffraction. ASTM Int. West Conshohocken.
21. Ghazimoradi, M., Safari, N., Soltanali, S., & Ghassabzadeh, H. (2023). Effect of simultaneous dealumination and metal incorporation of zeolite ZSM-5 on the catalytic performance in HTO process. *Microporous and Mesoporous Materials*, 112486, doi.org/10.1016/j.micromeso.2023.112486.
22. Karami, H., Soltanali, S., Najafi, A. M., Ghazimoradi, M., Yaghoobpour, E., & Abbasi, A. (2023). Amorphous silica-alumina as robust support for catalytic dehydrogenation of propane: Effect of Si/Al ratio on nature and dispersion of Cr active sites. *Applied Catalysis A: General*, 658, 119167, doi.org/10.1016/j.apcata.2023.119167.
23. Zhang, X., Cheng, D., Chen, F., & Zhan, X. (2017). n-Heptane catalytic cracking on hierarchical ZSM-5 zeolite: The effect of mesopores, *Chemical Engineering Science*, 168, 352–359, doi.org/10.1016/j.ces.2017.05.012.
24. Karami, H., Kazemeini, M., Soltanali, S., & Rashidzadeh, M. (2022b). The effect of post-synthesis modification of Faujasite zeolites (X, Y) on the catalytic performance of diesel hydrodesulfurization process, *Journal of Applied Research in Chemistry*, 15(4), 106–117, doi: 10.30495/jacr.2022.688740.
25. Najafi, A. M., Soltanali, S., & Ghassabzadeh, H. (2023). Enhancing the CO<sub>2</sub>, CH<sub>4</sub>, and N<sub>2</sub> adsorption and kinetic performance on FAU zeolites for CO<sub>2</sub> capture from flue gas by metal incorporation technique. *Chemical Engineering Journal*, 143719, doi.org/10.1016/j.cej.2023.143719.
26. Najafi, A. M., Soltanali, S., Khorashe, F., & Ghassabzadeh, H. (2023). Effect of binder on CO<sub>2</sub>, CH<sub>4</sub>, and N<sub>2</sub> adsorption behavior, structural properties, and diffusion coefficients on extruded zeolite 13X. *Chemosphere*, 324, 138275, doi.org/10.1016/j.chemosphere.2023.138275.
27. Karami, H., Kazemeini, M., Soltanali, S., & Rashidzadeh, M. (2022). Influence of adding a modified zeolite-Y onto the NiMo/Al<sub>2</sub>O<sub>3</sub> catalyst utilized to produce a diesel fuel with highly reduced sulfur content, *Microporous and Mesoporous Materials*, 332, 111704, doi.org/10.1016/j.micromeso.2022.111704.
28. Pérez-Ramírez, J., Verboekend, D., Bonilla, A., & Abelló, S. (2009). Zeolite catalysts with tunable hierarchy factor by pore-growth moderators. *Advanced Functional Materials*, 19(24), 3972–3979, doi.org/10.1002/adfm.200901394.
29. Sousa-Aguiar, E. F., Trigueiro, F. E., & Zotin, F. M. Z. (2013). The role of rare earth elements in zeolites and cracking catalysts. *Catalysis Today*, 218, 115–122, doi.org/10.1016/j.cattod.2013.06.021.
30. Zhang, D., Wei, Y., Xu, L., Chang, F., Liu, Z., Meng, S., Su, B.-L., & Liu, Z. (2008). MgAPSO-34 molecular sieves with various Mg stoichiometries: Synthesis, characterization and catalytic behavior in the direct transformation of chloromethane into light olefins. *Microporous and Mesoporous Materials*, 116(1–3), 684–692, doi.org/10.1016/j.micromeso.2008.06.001.
31. Zhan, W., Guo, Y., Gong, X., Guo, Y., Wang, Y., & Lu, G. (2014). Current status and perspectives of rare earth catalytic materials and catalysis, *Chinese Journal of Catalysis*, 35(8), 1238–1250, doi.org/10.1016/S18722067(14)60189.
32. Xue, N., Liu, N., Nie, L., Yu, Y., Gu, M., Peng, L., Guo, X., & Ding, W. (2010). 1-Butene cracking to propene over P/HZSM-5: Effect of lanthanum, *Journal of Molecular Catalysis A: Chemical*, 327(1–2), 12–19, doi.org/10.1016/j.molcata.2010.05.004.
33. Zhu, J., Yan, S., Qian, Y., Zhu, X., & Yang, F. (2023). Fabrication of fluffy-ball like ZSM-5 zeolite and its application in hexane catalytic cracking. *Microporous and Mesoporous Materials*, 351, 112465, doi.org/10.1016/j.micromeso.2023.112465.
34. Zhu, J., Yan, S., Xu, G., Zhu, X., & Yang, F. (2023). Fabrication of sheet-like HZSM-5 zeolites with various SiO<sub>2</sub>/Al<sub>2</sub>O<sub>3</sub> and process optimization in hexane catalytic cracking, *Journal of Solid State Chemistry*, 318, 123772, doi.org/10.1016/j.jssc.2022.123772.